

Time evolution of the reheating equation of state and its impact on the inflationary tensor perturbation spectrum

Avirup Ghosh^a and Deep Ghosh^b

^a*ARC Centre of Excellence for Dark Matter Particle Physics, School of Physics, The University of Melbourne, Victoria 3010, Australia*

^b*Department of Physical Sciences, Indian Institute of Science Education and Research, Kolkata, Mohanpur - 741246, India*

E-mail: avirup.ghosh1993@gmail.com, matrideb1@gmail.com

ABSTRACT: Among the very few available probes of the post-inflationary reheating epoch one is the spectrum of inflationary tensor perturbations which is affected by the Universe's equation of state during the reheating era. Contrary to the usual approach of assuming a constant equation of state during the reheating era, in this work, we have dynamically calculated the evolution of the reheating equation of state and find how it depends on the inflaton decay rate. We have also quantified its impact on the spectrum of the primordial tensor perturbations. Considering two different inflationary potentials of the E-model α -attractor class with $n=1(3)$ we have derived the evolution of the reheating equation of state for various values of the inflaton decay rate and also find that the inflationary tensor perturbations can be enhanced (suppressed) by a factor of $\sim 1.5-3$ compared to the usual calculations assuming a constant equation of state. This difference is attributed to the fact that the comoving horizon evolves differently in the two approaches and hence any particular comoving momentum mode enters the horizon at different instances and subsequently evolves differently.

Contents

1	Introduction	1
2	Dynamics of inflation and post-inflationary reheating	2
3	Propagation of tensor perturbations during reheating era	6
4	Summary	9
	References	9

1 Introduction

An era of exponential expansion at the beginning of the Universe, known as inflation, is necessary for explaining the large-scale homogeneity and isotropy of the present-day Universe. However, such an era eventually comes to an end giving rise to the standard radiation-dominated era, in order to match the predictions of the Big-Bang Nucleosynthesis (BBN). The epoch of inflaton energy transfer to the Standard Model radiation bath is known as reheating. The reheating era is the least understood era in the history of the early Universe, since, no direct probe of this era currently exists. However, several interesting phenomena such as the dark matter production, matter-antimatter asymmetry generation can happen during this epoch [1–4] and hence a proper understanding of the physics happening during this era is needed.

Apart from explaining the large-scale homogeneity and isotropy of the present-day Universe, inflation also acts as a natural origin of primordial perturbations [5–8] thereby providing explanation for the late-time structure formation through its scalar component. On the other hand, observations of the inflationary tensor perturbations or the inflationary gravitational waves (GW) can provide profound proof in favour of the slow-roll inflation. Recent detections of gravitational waves by LIGO [9], NANOGrav [10] etc. have led to several other proposals for GW detections over a wide range of frequencies [11–16].

The tensor perturbations generated during inflationary era exit the cosmological horizon during inflation and latter reenter the horizon and evolve through different phases of the Universe before ultimately reaching the present-day GW detectors. Moreover, gravity being very weakly interacting, GWs provide one of the cleanest signal to understand the physics of the early Universe. Several authors have already utilised this property to show that it is possible to unveil the physics of the reheating epoch through the observation of the primordial gravitational wave (GW) spectrum (see, for example, [17–21]).

Specifically, it has been pointed out that the equation of state (EOS) of the Universe ($w = p_{\text{tot}}/\rho_{\text{tot}}$) during the reheating era determines the shape of the primordial tensor perturbations spectra and with the advent of the next generation of GW detectors it is possible to determine the shape of this spectra thereby leading to a proper understanding of the physics occurring during this era [17–21]. The previous studies in this direction have considered the inflaton EOS w_ϕ to be a constant during reheating, but such an approximation is not always true. In fact, the shape of the inflationary potential can impact the inflaton EOS during the reheating era, and hence can also impact the propagation of tensor perturbations during this era. Moreover, the evolution of

the inflaton EOS for different values of inflaton decay rate may also be different and needs careful investigation.

With this motivation, we have considered two different inflationary potentials of the E-model α -attractor class and fixed the relevant parameters using the Cosmic Microwave Background (CMB) data of the scalar-spectral index n_s and the amplitude of the scalar perturbations A_s . Following which, we have solved the evolution equations of the inflaton energy density and radiation energy densities during reheating era to determine the time-evolution of the reheating EOS w_{RH} dynamically. This allows us to track the evolution of the comoving hubble radius ($1/aH$) during reheating era which impacts the spectra of primordial tensor perturbations produced during the inflationary epoch. Finally, we find that using the actual time-varying w_{RH} predicts a present-day GW spectrum which can be different from that obtained using a constant EOS by a factor of $\sim 1.5 - 3$.

This paper is organized as follows: In Sec. 2, we have obtained the evolutions of the reheating EOS and also the evolutions of comoving horizon of the Universe during the reheating era. Sec. 3 is devoted to determine the evolution of the tensor perturbations during reheating epoch and to obtain the impact of the time-variation of w_ϕ on the present-day GW spectrum. Lastly, in Sec. 4, we summarize and conclude.

2 Dynamics of inflation and post-inflationary reheating

Given a single-field potential $V(\phi)$, the inflationary dynamics is determined by the slow-roll parameters:

$$\epsilon(k_*) = \frac{M_{\text{Pl}}^2}{2} \left(\frac{V'(\phi)}{V(\phi)} \right)^2 \Big|_{\phi=\phi_*}, \eta(k_*) = M_{\text{Pl}}^2 \left(\frac{V''(\phi)}{V(\phi)} \right) \Big|_{\phi=\phi_*}, \quad (2.1)$$

where $'$ denotes derivative w.r.t ϕ , k_* is the CMB pivot scale 0.05 Mpc^{-1} and ϕ_* is the value of ϕ when k_* exits the horizon. These slow-roll parameters are directly related to the CMB observables, i.e., the scalar tilt n_s , amplitude of density perturbations A_s and the tensor-to-scalar ratio r , as follows:

$$n_s = 1 + 2\eta - 6\epsilon, A_s = \frac{1}{24\pi^2\epsilon} \frac{V(\phi)}{M_{\text{Pl}}^4}, r = 16\epsilon. \quad (2.2)$$

The recent Planck data [22] suggests $n_s = 0.9649 \pm 0.0044$, $A_s = (2.105 \pm 0.029) \times 10^{-9}$ and $r < 0.1$ at the pivot momentum $k_* = 0.05 \text{ Mpc}^{-1}$, which can be utilised to constrain the parameters of any given inflationary model.

While most of the monomial models of chaotic inflation fail to comply with the recent Planck data, the α -attractor models are one class of models that fit the current CMB data (see [23]) quite well. Apart from the consistency with the CMB data these models are also motivated from several theoretical perspectives. Most of these α -attractor models can actually arise from supergravity and can also explain supersymmetry breaking [24]. Additionally, the possible origin of the late time cosmological constant driven expansion can also be obtained within such models [25].

In this work, we have considered the general class of the E-model α -attractor potential:

$$V(\phi) = \lambda M_{\text{Pl}}^4 \left(1 - e^{-\sqrt{2/3}\alpha\phi/M_{\text{Pl}}} \right)^{2n} \simeq \left(\frac{2}{3\alpha} \right)^n \lambda M_{\text{Pl}}^4 (\phi/M_{\text{Pl}})^{2n}, \text{ about } \phi = 0 \quad (2.3)$$

for which,

$$n_s = \frac{1 - 2\left(1 + \frac{4n}{3\alpha}\right)e^{-\sqrt{2/3}\alpha\phi/M_{\text{Pl}}} + \left(1 - \frac{8n^2}{3\alpha}\right)e^{-2\sqrt{2/3}\alpha\phi/M_{\text{Pl}}}}{\left(1 - e^{-\sqrt{2/3}\alpha\phi/M_{\text{Pl}}}\right)^2}, \quad (2.4)$$

$$A_s = \frac{\alpha\lambda}{32n^2\pi^2} e^{2\sqrt{2/3}\alpha\phi/M_{\text{Pl}}} \left(1 - e^{-\sqrt{2/3}\alpha\phi/M_{\text{Pl}}}\right)^{2(1+n)}, \quad (2.5)$$

$$r = \frac{64n^2}{3\alpha} \frac{e^{-2\sqrt{2/3}\alpha\phi/M_{\text{Pl}}}}{\left(1 - e^{-\sqrt{2/3}\alpha\phi/M_{\text{Pl}}}\right)^2}. \quad (2.6)$$

Assuming $\alpha = 1$ and using the central values of n_s , A_s and $\epsilon(\phi_{\text{end}}) = r(\phi_{\text{end}})/16 = 1$, we obtain the parameters for two different potentials with $n = 1$ and $n = 3$ which are shown in tab. 1. At the end of inflation, $\epsilon(\phi_{\text{end}}) \simeq \frac{3}{2}\dot{\phi}^2/\rho_\phi|_{\phi_{\text{end}}} \sim 1$, $\dot{\phi} \sim \sqrt{V(\phi_{\text{end}})}$ and hence, $\rho_\phi \sim 3V(\phi_{\text{end}})/2 \equiv \rho_{\text{end}}$. We also assume the energy density in radiation, i.e., ρ_R , to be 0 at the end of inflation.

Model	λ	ϕ_k/M_{Pl}	$\phi_{\text{end}}/M_{\text{Pl}}$	r	N_k	a_{end}
E-model ($\alpha = 1, n = 1$) $\lambda M_{\text{Pl}}^4 \left(1 - e^{-\sqrt{2/3}\phi/M_{\text{Pl}}}\right)^2$ $\simeq \frac{1}{2} \frac{4}{3} \lambda M_{\text{Pl}}^4 (\phi/M_{\text{Pl}})^2$	1.12×10^{-10}	5.35	0.94	0.003	55	1.47×10^{-29}
E-model ($\alpha = 1, n = 3$) $\lambda M_{\text{Pl}}^4 \left(1 - e^{-\sqrt{2/3}\phi/M_{\text{Pl}}}\right)^6$ $\simeq \frac{8}{27} \lambda M_{\text{Pl}}^4 (\phi/M_{\text{Pl}})^6$	1.14×10^{-10}	6.67	1.83	0.003	56	5.03×10^{-29}

Table 1: Constraints imposed by the Planck CMB data ($n_s = 0.9649$, $A_s = 2.105 \times 10^{-9}$ at the pivot scale $k_* = 0.05 \text{ Mpc}^{-1}$) [22] on the parameters of the chosen inflationary potentials are presented. The inflation field start oscillation from $\phi = \phi_{\text{end}}$.

For $\phi < \phi_{\text{end}}$, the inflaton field ϕ starts oscillating about the minimum of $V(\phi)$, following the eq:

$$\ddot{\phi} + (3H + \Gamma)\dot{\phi} + V'(\phi) = 0, \quad (2.7)$$

where H is the hubble rate, $V'(\phi) = dV(\phi)/d\phi$ and Γ represents the decayrate of the inflaton condensate. Energy density and the pressure of the field ϕ are,

$$\rho_\phi = \frac{\dot{\phi}^2}{2} + V(\phi), \quad (2.8)$$

$$p_\phi = \frac{\dot{\phi}^2}{2} - V(\phi). \quad (2.9)$$

From the conservation of energy-momentum tensor:

$$\frac{d\rho_{\text{tot}}}{dt} + 3H(1 + w_{\text{RH}})\rho_{\text{tot}} = 0. \quad (2.10)$$

one obtains the evolution of the radiation energy density as follows,

$$\frac{d\rho_R}{dt} + 4H\rho_R = \Gamma(1+w_\phi)\rho_\phi, \quad (2.11)$$

where inflaton equation of state (EOS) $w_\phi = p_\phi/\rho_\phi$ and the reheating EOS w_{RH} is given by:

$$w_{RH} = \frac{w_\phi\rho_\phi + \rho_R/3}{\rho_\phi + \rho_R}, \quad (2.12)$$

assuming the Universe to be a two-fluid system during reheating era. On the other hand, from eqs. 2.7, 2.8 and 2.9, we get,

$$\frac{d\rho_\phi}{dt} + 3H(1+w_\phi)\rho_\phi = -\Gamma(1+w_\phi)\rho_\phi. \quad (2.13)$$

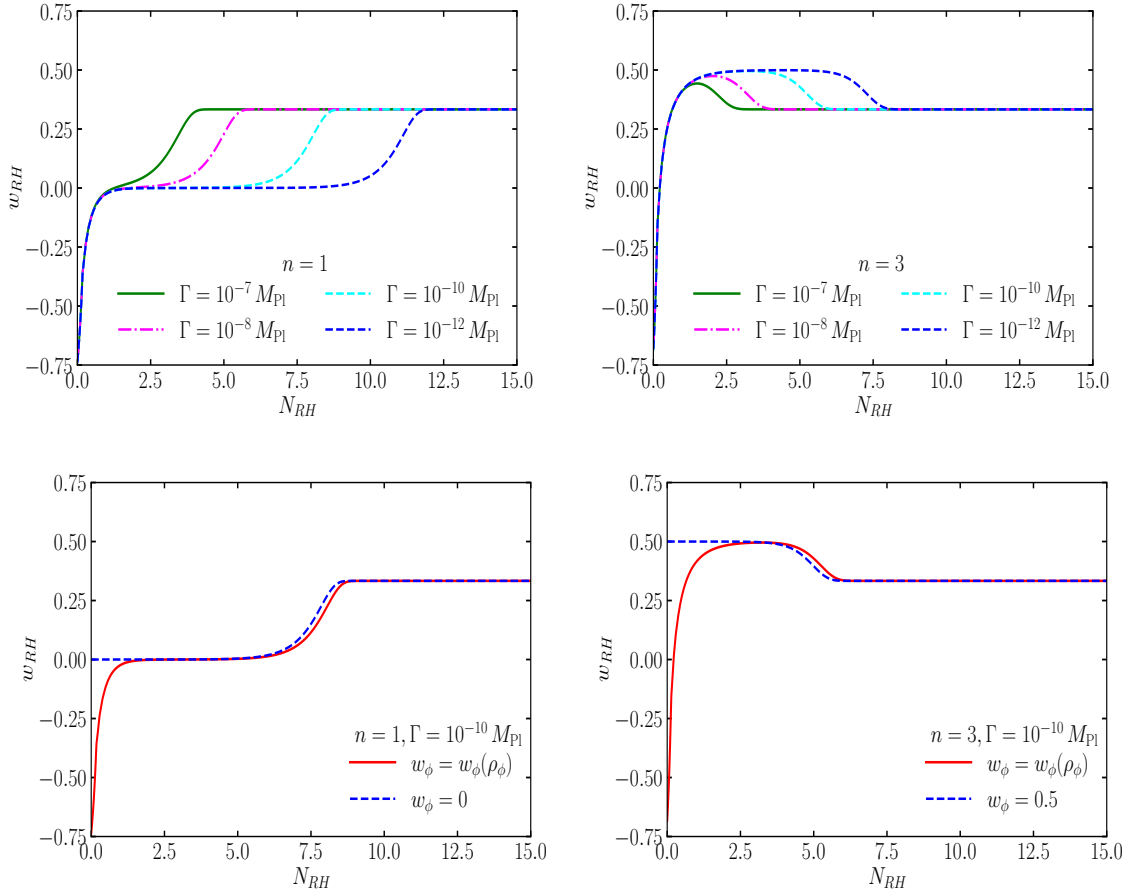


Figure 1: *Top:* Evolution of the reheating EOS w_{RH} during reheating era is shown as a function of the reheating e -foldings N_{RH} for the E-model α -attractor potential with $n = 1$ (left) and $n = 3$ (right). Here the four different values of the inflaton decayrate Γ have been considered. *Bottom:* Assuming $\Gamma = 10^{-10} M_{Pl}$, we have shown the evolutions of w_{RH} for constant EOS (blue dashed) and exact EOS (red solid) for E-model α -attractor potential with $n = 1$ (left) and $n = 3$ (right). See the text for details.

Therefore, eqs. 2.11 and 2.13 together imply that the dynamics of reheating is affected by the value of w_ϕ and following [26], w_ϕ is given by,

$$w_\phi(\rho_\phi) = 2 \frac{\int_{\phi_{m1}}^{\phi_{m2}} d\phi \sqrt{1 - V(\phi)/\rho_\phi}}{\int_{\phi_{m1}}^{\phi_{m2}} d\phi / \sqrt{1 - V(\phi)/\rho_\phi}} - 1, \quad (2.14)$$

where $\phi_{m1,m2}$ represent the amplitudes of inflaton oscillations during the reheating era. The formula in eq. 2.14 can capture the effects when inflationary potential is not absolutely symmetric around the minima of the Potential. For our chosen set of potentials, i.e.

$$\phi_{m1,m2}(\rho_\phi) = \sqrt{\frac{3}{2}} M_{\text{Pl}} \ln \left[\frac{1}{1 \pm \left(\frac{\rho_\phi}{\lambda M_{\text{Pl}}^4} \right)^{1/2n}} \right]. \quad (2.15)$$

Using eq. 2.14 we first obtain the inflaton EOS $w_\phi(\rho_\phi)$ as a function of the inflaton energy density ρ_ϕ and then use it to solve the eqs. 2.11 and 2.13. The resulting evolutions of ρ_ϕ and ρ_R are then used to obtain the reheating EOS w_{RH} from eq. 2.12. In the top panel of Fig. 1 we have shown the evolutions of w_{RH} for $n = 1$ (left) and $n = 3$ (right) for several values of the inflaton decayrate Γ .

Note that, if one approximates the potentials by the leading terms of their Taylor-series expansions about their corresponding minima, eq. 2.14 gives $w_\phi = 0$ for $n = 1$ and $w_\phi = 0.5$ for $n = 3$, respectively. We also solve eqs. 2.11 and 2.13 using these constant values of w_ϕ and hereafter refer this approach as the constant EOS approach. In the bottom panel of Fig. 1 we have compared the evolutions of w_{RH} as obtained in the actual EOS case (red solid) and in the constant EOS approach (blue dashed) for $n = 1$ (left) and $n = 3$ (right) assuming $\Gamma = 10^{-10} M_{\text{Pl}}$.

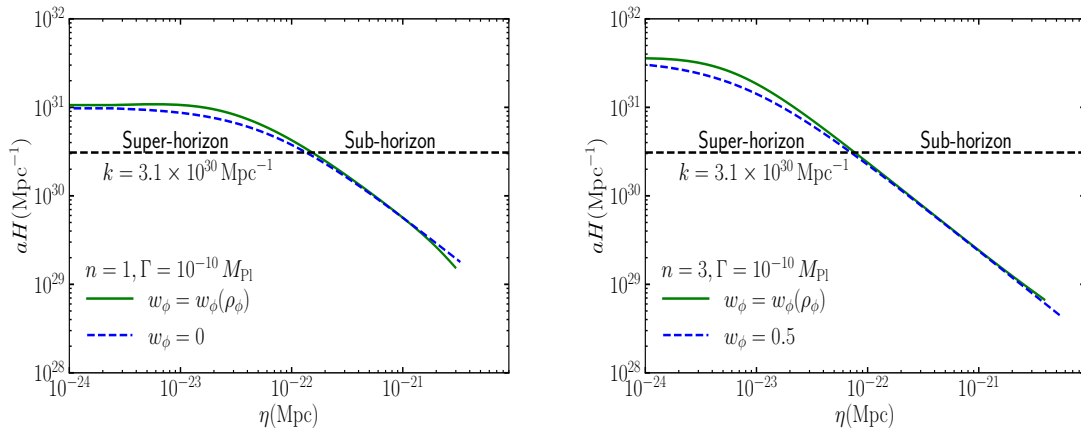


Figure 2: For the E-model α -attractor potential with $n = 1$ (left) and $n = 3$ (right), the evolution of aH have been shown as a function of the comoving time η . In each case, the blue dashed line shows the result obtained assuming a constant EOS and the green solid line shows the evolution when the actual EOS is considered. Here $\Gamma = 10^{-10} M_{\text{Pl}}$ is assumed. See the text for details.

As will be evident later, another quantity of interest for our study is the comoving horizon of the Universe during the reheating era. The inverse of the comoving horizon in the constant EOS case is given by,

$$aH(N) = \frac{a_{\text{end}} \sqrt{\rho_{\text{end}}}}{\sqrt{3} M_{\text{Pl}}} e^{-N(1+3w_\phi)/2}. \quad (2.16)$$

On the other hand, the same quantity for the actual EOS approach is obtained as follows,

$$aH(N) = \frac{a_{\text{end}}\sqrt{\rho_{\text{end}}}}{\sqrt{3}M_{\text{Pl}}} e^{N-3} \int_0^N dN' (1+w_{\text{RH}}(N')). \quad (2.17)$$

We have defined the end of reheating by the condition $\rho_\phi = \rho_R$. The differences of these quantities are evident from Fig. 2 where we have shown aH as a function of the comoving time $\eta = \int da/a^2 H$ for $n = 1$ (left) and $n = 3$ (right), respectively. In both the cases, we have considered $\Gamma = 10^{-10} M_{\text{Pl}}$ and have represented the results obtained for constant EOS by blue dashed lines while the result for actual EOS by the green solid lines. The black dashed line represents a particular comoving momentum $k = 3.1 \times 10^{30} \text{ Mpc}^{-1}$ which enters the horizon during the reheating era and hence will carry the imprints of the physics occurring during the reheating era.

3 Propagation of tensor perturbations during reheating era

As mentioned earlier, inflationary gravity waves (or tensor perturbations) provide new avenues to unveil the dynamics of reheating thanks to the current advancements in the field of GW detection [17–21]. During inflation, the comoving hubble radius ($1/aH$) decreases and any particular comoving momentum mode k of tensor perturbations produced during inflation become super-horizon when $k < aH$. After inflation, the comoving hubble radius ($1/aH$) increases and some of the super-horizon modes which earlier exited, reenter the horizon. After reentering the horizon such modes experience the effects of the evolution of the Universe and propagate following,

$$\ddot{h}_k + \frac{3\dot{a}}{a} \dot{h}_k + \frac{k^2}{a^2} h_k = 0, \quad (3.1)$$

in absence of any additional source term. In eq. 3.1, h_k represents the fourier transform of the amplitude of mode k and the polarization index is suppressed for brevity. When written in terms of the comoving time η , eq. 3.1 becomes,

$$h_k'' + 2aH h_k' + k^2 h_k = 0, \quad (3.2)$$

where $'$ denotes the derivative w.r.t η . From eq. 3.2, it is clear that for any given k , the evolution is governed by the evolution of $aH(\eta)$.

We define the transfer function and its derivative as, $\mathcal{T}_k(\eta) = h_k(\eta)/h_k^{\text{prim}}$ and $\mathcal{T}_k'(\eta) = h_k'(\eta)/h_k^{\text{prim}}$, respectively, with h_k^{prim} representing the amplitude of mode k at the horizon exit and solve eq. 3.2 to obtain

$$\begin{aligned} \mathcal{T}_k(\eta) &= \sqrt{\frac{2}{\pi}} k^{\left(\frac{3w_\phi-1}{3w_\phi+1}\right)} \left(\frac{\sqrt{3}M_{\text{Pl}}(1+3w_\phi)}{2a_{\text{end}}\sqrt{\rho_{\text{end}}}} + \eta \right)^{\left(\frac{3w_\phi-1}{3w_\phi+1}\right)} \\ &\quad \left(C_1 j_{\left(\frac{1-3w_\phi}{1+3w_\phi}\right)} \left(k \frac{\sqrt{3}M_{\text{Pl}}(1+3w_\phi)}{2a_{\text{end}}\sqrt{\rho_{\text{end}}}} + k\eta \right) + C_2 y_{\left(\frac{1-3w_\phi}{1+3w_\phi}\right)} \left(k \frac{\sqrt{3}M_{\text{Pl}}(1+3w_\phi)}{2a_{\text{end}}\sqrt{\rho_{\text{end}}}} + k\eta \right) \right), \\ \mathcal{T}_k'(\eta) &= -\sqrt{\frac{2}{\pi}} k^{\left(1+\frac{3w_\phi-1}{3w_\phi+1}\right)} \left(\frac{\sqrt{3}M_{\text{Pl}}(1+3w_\phi)}{2a_{\text{end}}\sqrt{\rho_{\text{end}}}} + \eta \right)^{\left(\frac{3w_\phi-1}{3w_\phi+1}\right)} \\ &\quad \left(C_1 j_{\left(\frac{2}{1+3w_\phi}\right)} \left(k \frac{\sqrt{3}M_{\text{Pl}}(1+3w_\phi)}{2a_{\text{end}}\sqrt{\rho_{\text{end}}}} + k\eta \right) + C_2 y_{\left(\frac{2}{1+3w_\phi}\right)} \left(k \frac{\sqrt{3}M_{\text{Pl}}(1+3w_\phi)}{2a_{\text{end}}\sqrt{\rho_{\text{end}}}} + k\eta \right) \right), \end{aligned}$$

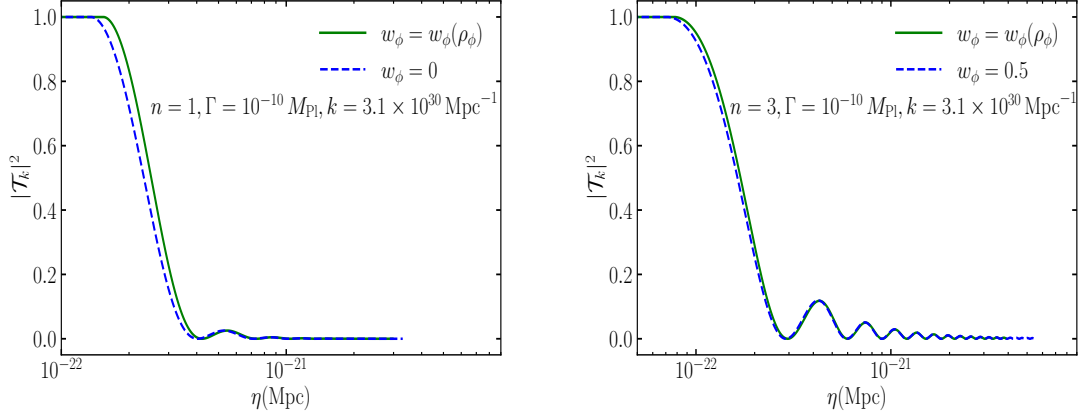


Figure 3: The evolution of a particular comoving momentum mode $k = 3.1 \times 10^{30} \text{ Mpc}^{-1}$ of tensor perturbations, that enters the horizon during reheating, is shown for $n = 1$ (left) and $n = 3$ (right) assuming constant EOS (blue dashed line) and actual EOS (green solid line), respectively. Here $\Gamma = 10^{-10} M_{\text{Pl}}$ is assumed. See the text for details.

for constant EOS case. Here j, y are the spherical bessel functions and the constants $C_{1,2}$ are defined as,

$$\begin{aligned} \begin{bmatrix} C_1 \\ C_2 \end{bmatrix} &= \sqrt{\frac{\pi}{2}} \left(\frac{1+3w_\phi}{2} \right)^{\left(\frac{3w_\phi-1}{3w_\phi+1} \right)} \begin{bmatrix} y\left(\frac{2}{1+3w_\phi}\right)\left(\frac{2}{1+3w_\phi}\right) \\ -j\left(\frac{2}{1+3w_\phi}\right)\left(\frac{2}{1+3w_\phi}\right) \end{bmatrix} \times \\ &\frac{1}{j\left(\frac{1-3w_\phi}{1+3w_\phi}\right)\left(\frac{2}{1+3w_\phi}\right)y\left(\frac{2}{1+3w_\phi}\right)\left(\frac{2}{1+3w_\phi}\right) - y\left(\frac{1-3w_\phi}{1+3w_\phi}\right)\left(\frac{2}{1+3w_\phi}\right)j\left(\frac{2}{1+3w_\phi}\right)\left(\frac{2}{1+3w_\phi}\right)}. \end{aligned} \quad (3.3)$$

On the other hand, in the case of actual EOS we have solved eq. 3.2 numerically using the results of aH as obtained in eq. 2.17 of Sec. 2.

Evolution of $|\mathcal{T}_k(\eta)|^2$ of the mode $k = 3.1 \times 10^{30} \text{ Mpc}^{-1}$ during reheating era are shown in Fig. 3 for $n = 1$ (left) and $n = 3$ (right), assuming, $\Gamma = 10^{-10} M_{\text{Pl}}$. Here, the blue dashed line shows the result for constant EOS and the green solid lines are obtained considering the actual evolution of w_{RH} . Clearly, the differences between the transfer functions obtained in the two different approaches stem from when a particular comoving momentum reenters the horizon and also from the instant of time signifying the end of the reheating era. As we shall see later, these can have substantial impact on the present-day spectrum of inflationary tensor perturbations.

After the end of reheating, the standard radiation domination takes over and the amplitude of tensor perturbations evolves as:

$$h_k^{\text{RD}}(\eta) = \sqrt{\frac{2}{\pi}} [C_1^k j_0(k\eta) + C_2^k y_0(k\eta)] h_k^{\text{prim}}. \quad (3.4)$$

We choose the coefficients $C_{1,2}^k$ such that at $\eta = \eta_{\text{RH}}$ our solutions for $\mathcal{T}_k(\eta_{\text{RH}})$ matches with eq. 3.4:

$$C_1^k = \sqrt{\frac{\pi}{2}} \left(\frac{y_1(k\eta_{\text{RH}})\mathcal{T}_k(\eta_{\text{RH}}) - y_0(k\eta_{\text{RH}})\mathcal{T}_k'(\eta_{\text{RH}})}{j_0(k\eta_{\text{RH}})y_1(k\eta_{\text{RH}}) - y_0(k\eta_{\text{RH}})j_1(k\eta_{\text{RH}})} \right), \quad (3.5)$$

$$C_2^k = -\sqrt{\frac{\pi}{2}} \left(\frac{j_1(k\eta_{\text{RH}})\mathcal{T}_k(\eta_{\text{RH}}) - j_0(k\eta_{\text{RH}})\mathcal{T}_k'(\eta_{\text{RH}})}{j_0(k\eta_{\text{RH}})y_1(k\eta_{\text{RH}}) - y_0(k\eta_{\text{RH}})j_1(k\eta_{\text{RH}})} \right). \quad (3.6)$$

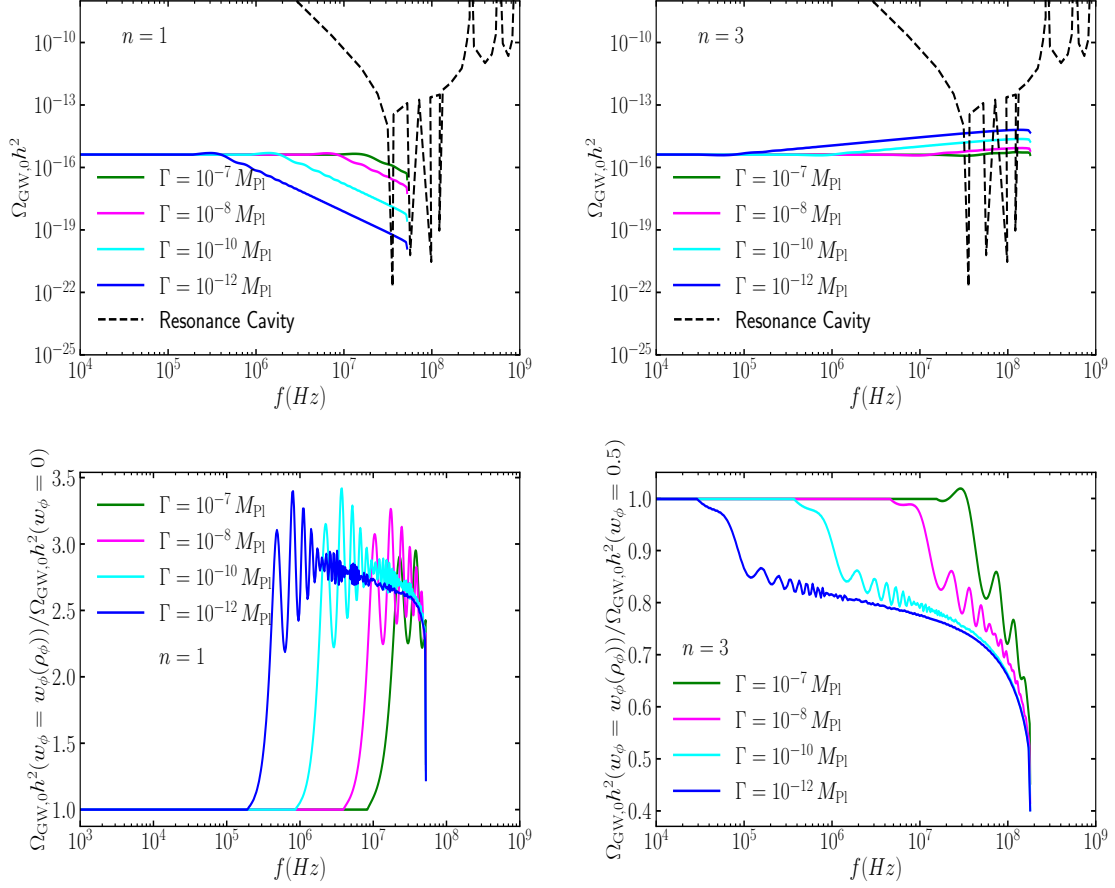


Figure 4: *Top:* The present day spectrum of inflationary gravitational waves (GW) for the E-model α -attractor potential with $n = 1$ (left) and $n = 3$ (right) are shown for different values of inflaton decayrate considering actual EOS. *Bottom:* The ratio of the GW energy density considering actual EOS to that obtained for constant EOS are shown for $n = 1$ (left) and $n = 3$ (right), for different values of Γ . See the text for details.

Similarly, at the matter-radiation equality, $\eta = \eta_{\text{eq}}$, it is made sure that the solutions smoothly transit to the solutions in matter-dominated era, given by:

$$h_k^{\text{MD}}(\eta) = \sqrt{\frac{2}{\pi}} \frac{\eta_{\text{eq}}}{\eta} [D_1^k j_1(k\eta) + D_2^k y_1(k\eta)] h_k^{\text{prim}}, \quad (3.7)$$

with

$$D_1^k = \left[C_1^k \left(\frac{3}{2k\eta_{\text{eq}}} - \frac{\cos(2k\eta_{\text{eq}})}{2k\eta_{\text{eq}}} + \frac{\sin(2k\eta_{\text{eq}})}{(k\eta_{\text{eq}})^2} \right) + C_2^k \left(1 - \frac{1}{(k\eta_{\text{eq}})^2} - \frac{\cos(2k\eta_{\text{eq}})}{(k\eta_{\text{eq}})^2} - \frac{\sin(2k\eta_{\text{eq}})}{2k\eta_{\text{eq}}} \right) \right], \quad (3.8)$$

$$D_2^k = \left[C_1^k \left(-1 + \frac{1}{(k\eta_{\text{eq}})^2} - \frac{\cos(2k\eta_{\text{eq}})}{(k\eta_{\text{eq}})^2} - \frac{\sin(2k\eta_{\text{eq}})}{2k\eta_{\text{eq}}} \right) + C_2^k \left(\frac{3}{2k\eta_{\text{eq}}} + \frac{\cos(2k\eta_{\text{eq}})}{2k\eta_{\text{eq}}} - \frac{\sin(2k\eta_{\text{eq}})}{(k\eta_{\text{eq}})^2} \right) \right]. \quad (3.9)$$

Ignoring the small period of dark energy domination in the late Universe, the amplitude of

tensor perturbations today (i.e., at $\eta = \eta_0$), is given by,

$$h_k(\eta_0) = \sqrt{\frac{2}{\pi}} \frac{\eta_{\text{eq}}}{\eta_0} [D_1^k j_1(k\eta_0) + D_2^k y_1(k\eta_0)] h_k^{\text{prim}}. \quad (3.10)$$

Using eq. 3.10 we obtain the spectral energy density today,

$$\frac{d\rho_{\text{GW}}}{d \ln k} = \frac{M_{\text{Pl}}^2}{4 a^2(\eta_0)} \sum_{+, \times} \frac{2k^3}{2\pi^2} \langle |h'_k(\eta_0)|^2 \rangle. \quad (3.11)$$

Using eq. 3.10 and introducing the definition of primordial power spectrum $\Delta_{k,\text{inf}}^2 = \sum_{+, \times} \frac{2k^3}{2\pi^2} \langle |h_k^{\text{prim}}|^2 \rangle$, eq. 3.11 can be re-expressed as,

$$\frac{d\rho_{\text{GW}}}{d \ln k} = \frac{M_{\text{Pl}}^2 k^2}{4 a^2(\eta_0)} \Delta_{k,\text{inf}}^2 \left\langle \left| \frac{dh_k(\eta)/h_k^{\text{prim}}}{d(k\eta)} \right|_{\eta=\eta_0}^2 \right\rangle, \quad (3.12)$$

where $\langle \dots \rangle$ represents average over multiple oscillations. The relative energy density in GW today is,

$$\Omega_{\text{GW}}^0 = \frac{1}{\rho_c} \frac{d\rho_{\text{GW}}}{d \ln k} = \frac{k^2}{12 a^2(\eta_0) H^2(\eta_0)} \Delta_{k,\text{inf}}^2 \left\langle \left| \frac{dh_k(\eta)/h_k^{\text{prim}}}{d(k\eta)} \right|_{\eta=\eta_0}^2 \right\rangle, \quad (3.13)$$

where the comoving momentum k has an one-to-one correspondence with the frequency of GW signal $f = k/2\pi a_0$. In our calculation of Ω_{GW}^0 (eq. 3.13) we have used $\eta_{\text{eq}} = a_{\text{eq}}/H_0 \sqrt{\Omega_{R,0}}$, $\eta_0 = \eta_{\text{eq}} \sqrt{\Omega_{M,0}/\Omega_{R,0}}$ and $H_0 = 100h \text{ km s}^{-1} \text{ Mpc}^{-1}$ with $h = 0.68$ [22].

The quantity $\Omega_{\text{GW}}^0 h^2$ for the E-model α -attractor potential with $n = 1$ and $n = 3$ are shown for different values of Γ in the top left and top right panels of Fig. 4, respectively. Clearly, as obtained in the constant EOS case, the GW spectrum is red-tilted for $n = 1$ and blue-tilted for $n = 3$. The ratio of $\Omega_{\text{GW}}^0 h^2$ for actual EOS to $\Omega_{\text{GW}}^0 h^2$ for constant EOS are presented in the bottom panel of Fig. 4 for several values of Γ . Here, it is clear that for $n = 1$ case (left) the GW spectrum is enhanced by a factor of ~ 3 while for $n = 3$ (right) case it is suppressed by a factor of ~ 1.5 . The black dashed curves show the sensitivity of the recently proposed resonance cavity experiments [27, 28] which may be effective in deciphering the high-frequency tail of the inflationary perturbation spectrum.

4 Summary

In this work we have considered two different classes of the E-model α -attractor inflationary potentials with $n = 1$ and $n = 3$, and studied the dynamics of the post-inflationary reheating era in two different approaches. In the first approach, the inflaton EOS is considered to be a constant, while, in the second approach, the proper evolution of the inflaton EOS has been taken into account. Apart from obtaining time evolution of the reheating EOS for different values of the inflaton decay rate we have also calculated how the propagation of primordial tensor perturbations are affected by this evolution of the reheating EOS. We found that the tensor perturbations can be enhanced/suppressed up to a factor of $\sim 1.5 - 3$ depending on the inflationary potential and inflaton decay rate. For both the models, the present-day gravitational wave spectrum are expected to fall within the sensitivity of the proposed resonance cavity experiments.

Acknowledgment

AG is funded by the Australian Research Council. AG and DG thanks Satyanarayan Mukhopadhyay for collaborating during the initial stage of the project.

References

- [1] K. Harigaya, M. Kawasaki, K. Mukaida, and M. Yamada, *Dark Matter Production in Late Time Reheating*, *Phys. Rev. D* **89** (2014), no. 8 083532, [[arXiv:1402.2846](#)].
- [2] Y. Mambrini and K. A. Olive, *Gravitational Production of Dark Matter during Reheating*, *Phys. Rev. D* **103** (2021), no. 11 115009, [[arXiv:2102.0621](#)].
- [3] D. S. Gorbunov and A. G. Panin, *Scalaron the mighty: producing dark matter and baryon asymmetry at reheating*, *Phys. Lett. B* **700** (2011) 157–162, [[arXiv:1009.2448](#)].
- [4] A. Dolgov, K. Freese, R. Rangarajan, and M. Srednicki, *Baryogenesis during reheating in natural inflation and comments on spontaneous baryogenesis*, *Phys. Rev. D* **56** (1997) 6155–6165, [[hep-ph/9610405](#)].
- [5] S. W. Hawking, *The Development of Irregularities in a Single Bubble Inflationary Universe*, *Phys. Lett. B* **115** (1982) 295.
- [6] A. H. Guth and S. Y. Pi, *Fluctuations in the New Inflationary Universe*, *Phys. Rev. Lett.* **49** (1982) 1110–1113.
- [7] A. A. Starobinsky, *Dynamics of Phase Transition in the New Inflationary Universe Scenario and Generation of Perturbations*, *Phys. Lett. B* **117** (1982) 175–178.
- [8] J. M. Bardeen, P. J. Steinhardt, and M. S. Turner, *Spontaneous Creation of Almost Scale - Free Density Perturbations in an Inflationary Universe*, *Phys. Rev. D* **28** (1983) 679.
- [9] **LIGO Scientific, Virgo** Collaboration, B. P. Abbott et al., *GW150914: The Advanced LIGO Detectors in the Era of First Discoveries*, *Phys. Rev. Lett.* **116** (2016), no. 13 131103, [[arXiv:1602.0383](#)].
- [10] **NANOGrav** Collaboration, N. S. Pol et al., *Astrophysics Milestones for Pulsar Timing Array Gravitational-wave Detection*, *Astrophys. J. Lett.* **911** (2021), no. 2 L34, [[arXiv:2010.1195](#)].
- [11] **KAGRA, Virgo, LIGO Scientific** Collaboration, R. Abbott et al., *Upper limits on the isotropic gravitational-wave background from Advanced LIGO and Advanced Virgo’s third observing run*, *Phys. Rev. D* **104** (2021), no. 2 022004, [[arXiv:2101.1213](#)].
- [12] M. Branchesi et al., *Science with the Einstein Telescope: a comparison of different designs*, *JCAP* **07** (2023) 068, [[arXiv:2303.1592](#)].
- [13] J. Crowder and N. J. Cornish, *Beyond LISA: Exploring future gravitational wave missions*, *Phys. Rev. D* **72** (2005) 083005, [[gr-qc/0506015](#)].
- [14] N. Seto, S. Kawamura, and T. Nakamura, *Possibility of direct measurement of the acceleration of the universe using 0.1-Hz band laser interferometer gravitational wave antenna in space*, *Phys. Rev. Lett.* **87** (2001) 221103, [[astro-ph/0108011](#)].
- [15] P. Amaro-Seoane et al., *Low-frequency gravitational-wave science with eLISA/NGO*, *Class. Quant. Grav.* **29** (2012) 124016, [[arXiv:1202.0839](#)].
- [16] G. Janssen et al., *Gravitational wave astronomy with the SKA, PoS AASKA14* (2015) 037, [[arXiv:1501.0012](#)].
- [17] S. Kuroyanagi, T. Chiba, and N. Sugiyama, *Precision calculations of the gravitational wave background spectrum from inflation*, *Phys. Rev. D* **79** (2009) 103501, [[arXiv:0804.3249](#)].
- [18] D. G. Figueroa and E. H. Tanin, *Ability of LIGO and LISA to probe the equation of state of the early Universe*, *JCAP* **08** (2019) 011, [[arXiv:1905.1196](#)].
- [19] M. R. Haque, D. Maity, T. Paul, and L. Sriramkumar, *Decoding the phases of early and late time reheating through imprints on primordial gravitational waves*, *Phys. Rev. D* **104** (2021), no. 6 063513, [[arXiv:2105.0924](#)].

- [20] S. S. Mishra, V. Sahni, and A. A. Starobinsky, *Curing inflationary degeneracies using reheating predictions and relic gravitational waves*, *JCAP* **05** (2021) 075, [[arXiv:2101.0027](#)].
- [21] A. K. Soman, S. S. Mishra, M. Shafi, and S. Basak, *Inflationary Gravitational Waves as a probe of the unknown post-inflationary primordial Universe*, [arXiv:2407.0795](#).
- [22] **Planck** Collaboration, N. Aghanim et al., *Planck 2018 results. VI. Cosmological parameters*, *Astron. Astrophys.* **641** (2020) A6, [[arXiv:1807.0620](#)]. [Erratum: *Astron. Astrophys.* 652, C4 (2021)].
- [23] **Planck** Collaboration, Y. Akrami et al., *Planck 2018 results. X. Constraints on inflation*, *Astron. Astrophys.* **641** (2020) A10, [[arXiv:1807.0621](#)].
- [24] R. Kallosh and A. Linde, *Planck, LHC, and α -attractors*, *Phys. Rev. D* **91** (2015) 083528, [[arXiv:1502.0773](#)].
- [25] E. V. Linder, *Dark Energy from α -Attractors*, *Phys. Rev. D* **91** (2015), no. 12 123012, [[arXiv:1505.0081](#)].
- [26] M. S. Turner, *Coherent Scalar Field Oscillations in an Expanding Universe*, *Phys. Rev. D* **28** (1983) 1243.
- [27] N. Herman, A. Füzfa, L. Lehoucq, and S. Clesse, *Detecting planetary-mass primordial black holes with resonant electromagnetic gravitational-wave detectors*, *Phys. Rev. D* **104** (2021), no. 2 023524, [[arXiv:2012.1218](#)].
- [28] N. Herman, L. Lehoucq, and A. Füzfa, *Electromagnetic antennas for the resonant detection of the stochastic gravitational wave background*, *Phys. Rev. D* **108** (2023), no. 12 124009, [[arXiv:2203.1566](#)].